Korean J. Chem. Eng., **30**(4), 836-841 (2013)
DOI: 10.1007/s11814-013-0008-9

TiO_2 nanotube-supported V_2O_5 catalysts for selective NO reduction by NH_3

Liyuan Xiong, Qin Zhong†, Qianqiao Chen, and Shule Zhang

School of Chemical Engineering, Nanjing University of Science and Technology, Nanjing 210094, P. R. China
(*Received 14 August 2012 • accepted 15 January 2013*)

Abstract−TiO_2 nanotubes (TNT) were prepared by hydrothermal method at 140 °C for 23 h. The V_2O_5/TNT (VTNT) catalysts were obtained by impregnation in NH_4VO_3 solution. The VTNTs exhibited much higher denitration efficiency than those supported on the raw TiO_2, and satisfactory resistance to water and sulfur. Results from BET, TEM, XRD, NH_3-TPD and EPR verified that V_2O_5 was dispersed well on TNT, thus favoring NH_3 adsorption, promoting the transformation from V^{5+} to V^{4+}, conducing to the formation of oxygen vacancies and superoxide radicals in the presence of NH_3 and O_2, and then resulting in the high catalytic activity of VTNTs.

Key words: TNT, V_2O_5, Hydrothermal, Dispersion, SCR

INTRODUCTION

Nitrogen oxides (NO_x) contribute to a variety of harmful environmental effects such as acid rain, photochemical smog and ozone depletion [1,2]. Selective catalytic reduction (SCR) of NO_x by NH_3 in the presence of O_2 remains one of the most effective processes for the removal of NO [3,4]. V_2O_5/TiO_2 and V_2O_5-WO_3/TiO_2 (anatase) catalysts operated at 350-400 °C, with less than 1% V_2O_5 loading, have been widely accepted as commercial catalysts [5-7]. To make full use of high temperature flue gas, the denitration unit has to be located upstream of the electrostatic precipitator and desulfurization. However, the flue gas without dust removal contains a high concentration of fly ash (e.g., K_2O, CaO and As_2O_3), which reduces catalytic performance and shortens the lifetime of catalysts [8,9]. In addition, high temperature can cause a series of side reactions, such as the oxidation of NH_3 into NO, the formation of N_2O, and the agglomeration of catalysts [10]. Therefore, it is essential to develop superior SCR catalysts with high activity at low temperature (<250 °C) to avoid those drawbacks.

The V_2O_5/TiO_2 catalysts system has advantages of mature technology, high selectivity and good resistance to water and sulfur, compared with other catalysts. It has been extensively studied in order to improve the catalytic activity at low temperature, reduce cost in industry application, raise economical benefits and provide the modification of other catalyst system with guidance and direction. Other metal oxides such as WO_3, MoO_2 and CeO_2 were adopted as promoters to improve catalysts' properties [11-13]. Non-metal doped vanadium catalysts were developed to increase the amount of surface superoxide radical by lattice distortion [14,15]. The modification of carriers was also investigated, such as TiO_2-ZrO_2 [16], TiO_2-SiO_2 [17], carbon nanotubes [18], and activated carbon fibers (ACF) [19].

TiO_2 has been extensively applied as support for its low cost, extensive sources, non-toxicity, stability and the resistance of SO_2 [20-22], so we targeted the modification of TiO_2 carrier. In general, high specific surface area can promote the dispersion of the active species and then improve the catalytic activity [23]. Thus, increasing the surface area of TiO_2 becomes a possible approach to improve the catalytic activity under low temperature. TNT has much larger surface area than nanoparticles and nanometer films. Moreover, it possesses fine mechanical properties and good chemical stability. Hydrothermal synthesis is a promising method to synthesize TNT for its facility and low cost; furthermore, it's easy to achieve desirable morphology by controlling processing parameters [24]. Synthesized with hydrothermal treatment in alkaline solution, TNT has large specific surface area, uniform diameter, fine purity and high adsorptive capacity. Our work focuses on the application of TNT on SCR catalysts, and illustrating the function of TNT in improving the catalytic activity of vanadium catalysts.

EXPERIMENTAL

1. Preparation

TNT was synthesized with a similar method to that reported by Kasuga et al. [25]. 6 g TiO_2 nanopowder (Commercial titanium pigment, Nanjing High Technology of Nano Material Co. Ltd.) was hydrothermally treated with 10 M NaOH aqueous solution (100 mL), sealed in a Teflon autoclave (200 mL) and heated at 140 °C for 23 h. The slurry was first washed with deionized water until neutral, and then immersed into 0.1 M HNO_3 aqueous solution for 24 h. The slurry was scoured with deionized water until neutral again, and then filtered. Whereafter, the samples were dried at 80 °C overnight, and then calcined at 350 °C, 400 °C, 450 °C, 500 °C, denoted as TNT-350, TNT-400, TNT-450, TNT-500, respectively. VTNT catalysts were prepared by impregnation in proper quantities of NH_4VO_3 solution with heating and agitating for 1 h to acquire catalysts with 1 wt% V_2O_5 loading. The products were dried at 120 °C, and then calcined at 350 °C, labeled as VTNT-350, VTNT-400, VTNT-450, VTNT-450, respectively.

2. Activity Test

Research on selective catalytic reduction of NO with NH_3 was conducted over a fixed-bed reactor (i.d. 6.8 mm) at 120-300 °C under normal pressure. The fixed bed packed with 0.5 g catalyst particles (20-40 mesh) with a type K thermocouple was placed at the center to monitor temperature. The gas flow was all controlled by mass

†To whom correspondence should be addressed.
E-mail: zq304@mail.njust.edu.cn

flow controllers (SY-9303B). The feeding gas mixture consisted of 800 ppm NO, 800 ppm NH_3, 4 vol% O_2, 400 ppm SO_2 (when used), and 4 vol% H_2O (when used), balanced with N_2 to reach a total flow rate of 150 mL/min. The GHSV was 16,521 h^{-1}. Before testing, the catalyst sample was preabsorbed by the reaction mixture for 2 h to avoid the influence of NO adsorption. The concentrations of NO_x at the inlet and outlet were analyzed by a flue gas analyzer (MRU Vario Plus). Concentration measurement was carried out after the reaction system was maintained for 1 h at each sampling temperature. The NO_x conversion was defined as follows:

$$NO_x \text{ conversion} = \frac{NO_{x,in} - NO_{x,out}}{NO_{x,out}} \times 100\% \quad (1)$$

3. Characterization

The BET surface areas were determined by N_2 adsorption with a V-Sorbet 2800S automated gas sorption apparatus at −196 °C. The morphology was observed through a JEM-2100 transmission electron microscope (TEM). Before TEM observation, the samples were re-dispersed in ethanol by ultrasonic treatment and dropped on carbon-copper grids. The X-ray diffraction (XRD) measurements were performed on a XD-3 diffractometer equipped with Cu-K_α radiation (λ=0.15418 nm) in the 2θ range of 10-80° using a step size of 0.02°, the tube voltage was 35 kV, and the current was 20 mA. The NH_3 temperature programmed desorption (NH_3-TPD) experiment was all carried out on a Quanta Chembet 3000 with 200 mg of each catalyst, and N_2 was used as the carrier gas. The flow rate of the system was kept at 70 mL/min with the heating rate of 15 °C/min from 60 °C up to 700 °C. Before NH_3-TPD test, all the samples were dried at 120 °C for 6 h. The electron paramagnetic resonance (EPR) measurements were made with a Bruker EMX-10/12-type spectrometer in the X-band, the powder samples were tested at ~9.76 GHz under room temperature before and after the co-adsorption of NH_3 and O_2, and all the samples were 100 mg.

RESULTS AND DISCUSSION

1. Catalytic Activity

The activities of V_2O_5/TiO_2 ($VTiO_2$) calcined at 350 °C and VTNTs are presented in Fig. 1 for comparison. Obviously, the catalytic activity of VTNT-350 was much higher than that supported on the raw TiO_2. Although their NO_x conversion both generally increased with the reaction temperature, the conversion of VTNT-350 elevated dramatically after 180 °C, and that of $VTiO_2$ increased smoothly until 240 °C. When the temperature reached 270 °C, the NO_x removal rate of VTNT-350 had already risen up to 93.05%, and that of $VTiO_2$ was just 54.90%. It was noteworthy that the denitration efficiency decreased with the increase of TNT's calcination temperature, especially after calcining at 450 °C, the activity of VTNT-450 declined sharply, and was closely approximated to that of $VTiO_2$. Linking up with BET results and TEM images, the higher activity of VTNTs was associated with the good dispersion of V_2O_5 on TNT.

2. Durability Test

Because the catalytic activity over VTNTs declined with calcination temperature increasing, it was essential to investigate thermal behaviors of the two catalysts experimentally. The experimental conditions were the same as that of the activity test, and the NO_x conversion was recorded every 5 h. Fig. 2 shows the activity evolution of VTNT-350 and $VTiO_2$ with time at 300 °C. The deNO_x activity for both of the catalysts maintained at the initial value after 120 h. It indicated that despite being affected greatly by calcination temperature, VTNT-350 had good thermal stability at 300 °C.

3. Catalyst Characterization

3-1. TEM

Treated in alkali solution hydrothermally, Ti-O-Ti bonds of TiO_2 ruptured to form intermediates containing Ti-O-Na or Ti-OH bonds. These intermediates rearranged to form sheets of edge-sharing TiO_6 octahedron with Na^+ and OH^- intercalating into the sheets. Through Na^+ exchange with H^+ by acid washing or dipping, titanic acid nanotube (TAN) formed [26-28]. Subsequently, we could acquire TNT after heat treatment of TAN. Fig. 3 exhibits the TEM images of TiO_2, TAN, VTNT-350 and VTNT-450. As is shown in Fig. 3(a), the raw TiO_2 consisted of granular crystals with an average diameter of 20 nm. In Fig. 3(b), the product synthesized via hydrothermal treatment possessed multi-layered hollow tubular structure with diameter in the range of 8-12 nm. There were no nanoparticles that adhered to TAN, but rather a few sheets still mixed with those nanotubes. Fig. 3(c) shows that VTNT-350 catalyst, after heat treatment and

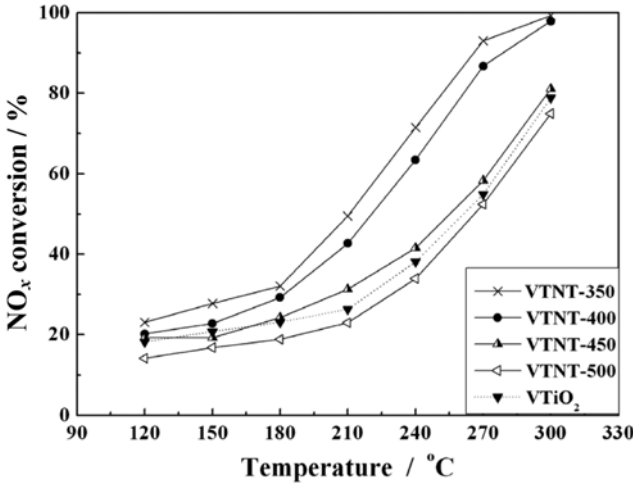

Fig. 1. NO_x conversion over $VTiO_2$ and VTNTs calcined at different temperature.

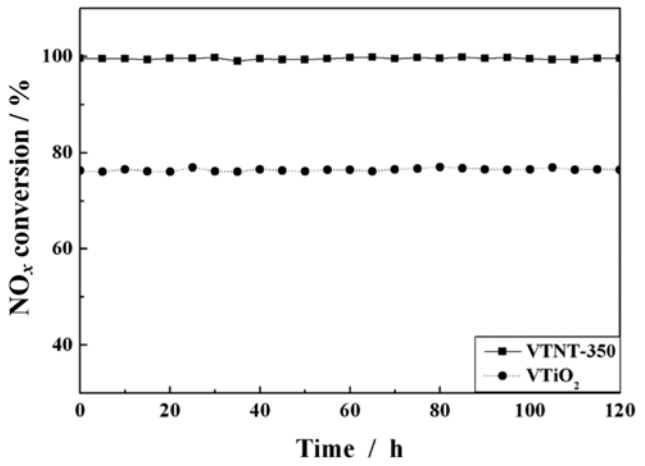

Fig. 2. The comparison of thermal stability over VTNT-350 and $VTiO_2$.

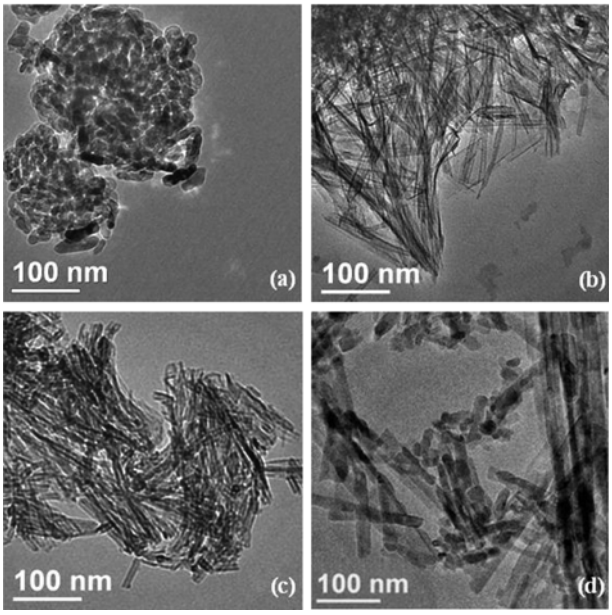

Fig. 3. TEM images of TiO_2, TAN, and VTNT-350 catalyst.
(a) TiO_2; (b) TAN; (c) VTNT-350; (d) VTNT-450

impregnation of V species, still retained good tubular configuration. The hollow structure of TiO_2 nanotubes could provide abundant pore path that benefited the dispersion of V_2O_5 and raised the denitration efficiency. Furthermore, no bulky particles aggregating on tube wall was observed. This demonstrated that the active component was well dispersed over the TNT support. When TNT was calcined at 450 °C, all the nanotubes unfolded into sheets, and some sheets further fractured to the same particles as the raw TiO_2, as shown in Fig. 3(d). It might be the primary reason why the catalytic activity of VTNT-450 was closed to $VTiO_2$, rather than VTNT-350.

3-2. XRD

The XRD patterns of TAN, $VTiO_2$ and VTNTs calcined at different temperature are depicted in Fig. 4. TAN without any heat treatment appeared vague peaks at 2θ of 24.5° and 48.6° corresponding to octahedron of $H_2Ti_2O_5 \cdot H_2O$ (JCPDS: 47-0124) [29]. As calcination temperature of TNT rose up to 400 °C, the peaks moved to 25.3° and 48.2° respectively, with the crystal transition from orthorhombic phase to amorphous TiO_2 as it shown in Fig. 4(a)-4(d). It caused the coexistence of TAN and TNT in the XRD pattern under the relative low calcining temperature. When the temperature reached 450 °C, there were peaks around 25°, 38°, 48°, 54° and 55° corresponding to (101), (004), (200), (105) and (211) of anatase phase (JCPDS: 21-1272) accompanied with the dilapidation and coagulation of nanotubes [29,30]. And the emergence of obvious anatase peaks demonstrated good crystallinity of VTNT and the rupture of tubular structure, leading to the sudden decline of VTNTs' catalytic activity. Moreover, as calcination temperature increased, layer structure of nanotubes disappeared, and the anatase peaks of VTNT became sharper and sharper, as well as the peak intensity got stronger, confirming that the crystalline degree and size of VTNT increased gradually with the increase of calcining temperature according to Scherrer's equation. Compared with $VTiO_2$, VTNT-350 had even larger half peak width, implying that its grain size was smaller and the specific surface area was much higher, in accord with the BET results. In none of the samples appeared the peak of V_2O_5, indicating that the crystallite size of V oxides was too small to be detected by the diffraction, or V_2O_5 was well dispersed on TNT. The result was consistent with the observation of TEM.

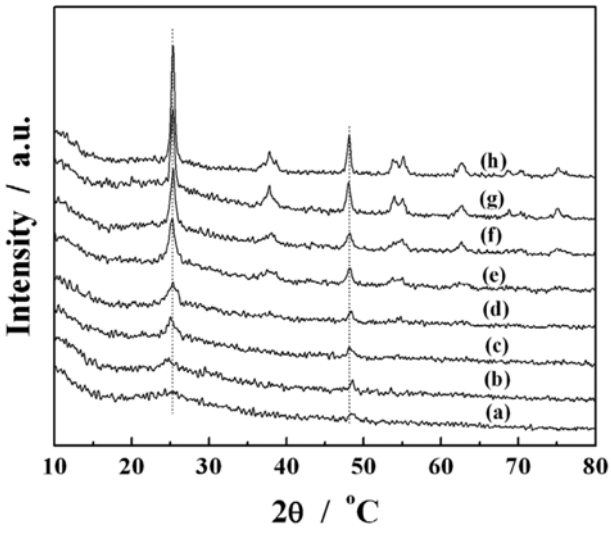

Fig. 4. XRD patterns of TAN, $VTiO_2$ and VTNTs calcined at different temperature.
(a) TAN; (b) VTNT-250; (c) VTNT-350; (d) VTNT-400; (e) VTNT-450; (f) VTNT-500; (g) VTNT-600; (h) $VTiO_2$

3-3. BET

The surface area of carriers played an important role in the dispersion of active species that could improve the catalytic activity [31]. The S_{BET} of TAN without calcination, synthesized from the raw TiO_2 with hydrothermal treatment, soared to 365 m^2/g, which was four times as large as that of the raw TiO_2, as shown in Table 1. The pore volume of TAN increased from 0.26 of the raw TiO_2 to 0.92 cm^3/g. After calcining, the S_{BET} of TNT-350 decreased sharply to 222 m^2/g, and the S_{BET} declined along with increasing calcination temperature, and so did the pore volume. This mainly resulted from the tubular structure ruptured by calcination. However, the S_{BET} scarcely decreased, when VTNT and $VTiO_2$ were loaded with a small amount of vanadium; meanwhile, the pore volume gained a little. This indicated that the V species was indeed loaded on the TNT support and got good dispersion without agglomeration or blocking. VTNT-350 had larger S_{BET} and its pore size distribution was more uniform than $VTiO_2$, leading to the improvement of the catalytic activity.

Although VTNT-450's S_{BET} was still two times of $VTiO_2$, its denitration efficiency declined to the degree of $VTiO_2$. We speculated from

Table 1. BET results of TAN, TiO_2, $VTiO_2$ and VTNTs

Sample	S_{BET} ($m^2\ g^{-1}$)	Pore volume ($cm^3\ g^{-1}$)	Pore size (nm)
TAN	365	0.92	10.6
TiO_2	88	0.26	20.0
$VTiO_2$	87	0.41	15.8
TNT-350	222	0.80	10.8
VTNT-350	210	0.99	15.5
VTNT-450	176	0.75	16.4

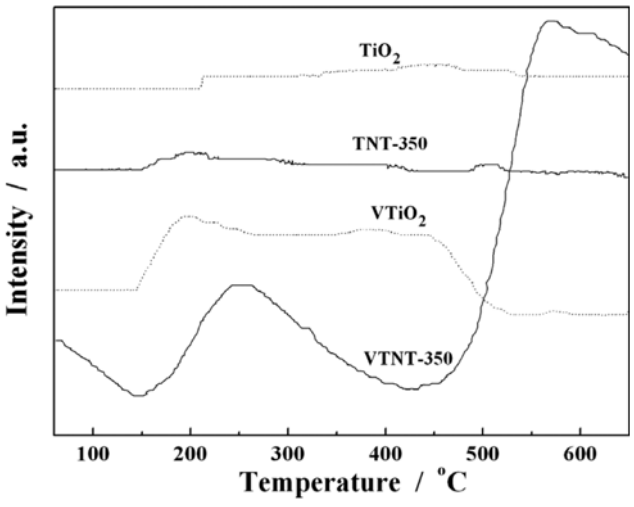

Fig. 5. NH_3-TPD profiles of TNT-350, TiO_2, VTNT-350 and $VTiO_2$.

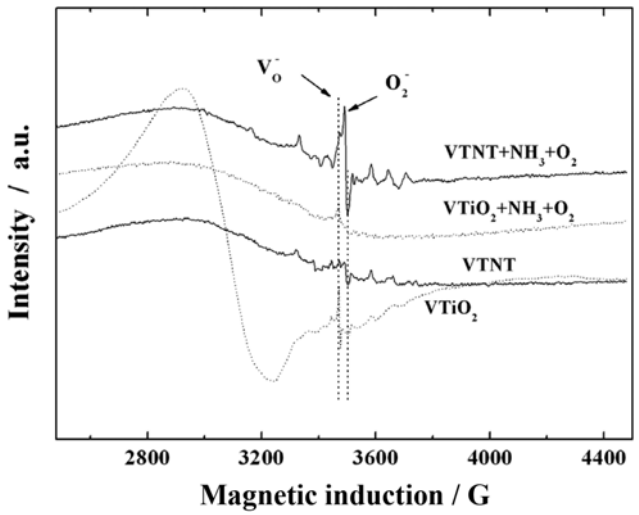

Fig. 6. EPR curves of VTNT-350 and $VTiO_2$ before and after aeration with NH_3 and O_2.

the TEM and XRD characterization that the nanotubes were destroyed by calcination at such high temperature, resulting in most active sites sintering. As a result, the NO_x removal was as low as that of $VTiO_2$.

3-4. NH_3-TPD

In fact, it was widely accepted that NH_3 adsorption and activation was not only the first step but also the essential one for the SCR reaction [32,33]. The strong surface acidity of catalysts was required to ensure sufficient NH_3 adsorption and further activation [34]. Therefore, we compared the surface acidity of VTNT-350 with $VTiO_2$ by NH_3-TPD testing, and further investigated the dispersion of V_2O_5 on the two different carriers and its internal connection with catalytic activity. Closely related to the dispersion of V species on the support, NH_3 was mainly absorbed on both Brønsted and Lewis acid sites of V_2O_5 (0 1 0) surface [32]. To avoid the influence of the supports, the NH_3 adsorption ability of TNT-350 and TiO_2 was also examined. As seen from Fig. 5, there were no obvious desorption peaks for both TNT-350 and TiO_2, the NH_3 desorption peaks only arose after V_2O_5 loaded on the carrier surface, indicating that NH_3 reacted or was adsorbed only on the active sites of V species. The TPD curves of VTNT-350 were quite different from $VTiO_2$. A small amount of ammonia was desorbed from $VTiO_2$ with two desorption peaks centering at 200 and 450 °C, and the whole desorption process had terminated before 530 °C. In contrast, there were two broad desorption peaks with high intensity appearing at 260 and 570 °C for VTNT-350, respectively. Unfortunately, limited by the test instrument, we couldn't observe the integral peak shape. However, it was enough to illuminate that the VTNT-350 owned higher amount of strongly bonded ammonia compared with $VTiO_2$, namely VTNT-350 with fine dispersion of active component on TNT possessed more strong solid acid sites in favor of denitration reaction. The NH_3-TPD profiles revealed that the fine dispersion of V_2O_5 on the TNT support reinforced surface acidity of catalysts, favored NH_3 adsorption and activation, and then drove the transform of V^{5+} to V^{4+}, resulting in the improvement of catalytic activity, according to the Eley-Rideal mechanism [35].

3-5. EPR

To further explore the promotion of catalytic activity by good dispersion under reaction atmosphere, the EPR spectra of VTNT-350 and $VTiO_2$ catalysts was measured before and after aeration with mixed gas of 800 ppm NH_3 and 4% O_2 at 240 °C for 2 h. V^{5+} with $3d^0$ electronic configuration was EPR silent due to the absence of unpaired electron, while V^{4+} with $3d^1$ was EPR sensitive splitting into eight hyperfine peaks [36]. As shown in Fig. 6, the hyperfine signal of V^{4+} in VTNT-350 was clearer and stronger than that in $VTiO_2$ before aeration, indicating that V_2O_5 got good dispersion on TNT. In the case of VTNT-350, the signal of V^{4+}, superoxide radical (O_2^-) and oxygen vacancy (V_O^-) was boosted sharply after the co-adsorption of NH_3 and O_2. Nevertheless, as to $VTiO_2$, the obvious signal of Ti^{3+} disappeared, the signal of V^{4+} was very weak and the signal of superoxide radical and oxygen vacancy hardly changed. The fine dispersion of V_2O_5 raised the surface acidity of VTNT-350, promoted NH_3 adsorption and activation on the TNT carrier. NH_3 as electron donor could reduced V^{5+} to V^{4+} (even further reduction to V^{3+} in principle), generated more oxygen vacancy simultaneously [37]. O_2 captured an electron from low valent metal ions or oxygen vacancy (which could captured electron from adjacent metal ions), and then brought in more superoxide radical, which was beneficial to the formation of NO_2^- and NO_3^- promoting low temperature SCR reaction. The tremendous increase in oxygen vacancy and superoxide radical's signal of VTNT-350 under NH_3 and O_2 stream, was mainly because of NH_3 abundant adsorption and strong activation on the surface of VTNT-350 closely connected with the good dispersion of V species, and eventually resulted in the increase of the NO_x removal.

4. Effect of SO_2 and H_2O on the Catalysts

To value the possibility of VTNT on industrial application, we investigated its resistance to sulfur and water poisoning, and for the sake of comparison, the water and sulfur resistance over $VTiO_2$ was also studied. Fig. 7 displays the evolution of catalytic activity over VTNT-350 and $VTiO_2$ with the addition of 4 vol% H_2O, 400 ppm SO_2, and 4 vol% H_2O+400 ppm SO_2 into the feed stream at 240 and 270 °C, respectively. When SO_2 was introduced into the feed, the denitration efficiency of VTNT-350 at 240 and 270 °C both gradually increased by about 5%, that of $VTiO_2$ only increased by about

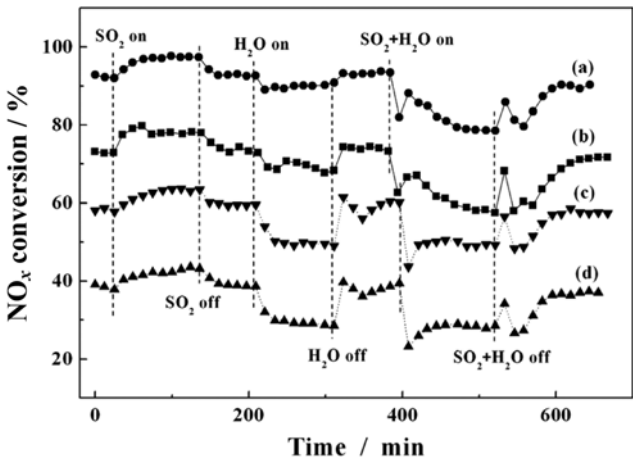

Fig. 7. Evolution of NO_x conversion over VTNT-350 and $VTiO_2$ in the presence of 4 vol% H_2O, 400 ppm SO_2, and 4 vol% H_2O+400 ppm SO_2 at 240 and 270 °C.
(a) VTNT-350 at 270 °C; (b) VTNT-350 at 240 °C; (c) $VTiO_2$ at 270 °C; (d) $VTiO_2$ at 240 °C

3%, and all the NO_x conversion reached stable state over a period of time. When the SO_2 provision was shut off, the NO_x removal efficiency dropped back to original level along with the consumption of intermediates good for denitration reaction. It manifested that SO_2 participated in the reaction, and the intermediates during the reaction process promoted the NO_x removal to a certain degree. This promotion was not unique, Long et al. [38] and Zhu et al. [39] thought that the promoting by SO_2 might be due to the formation of surface SO_4^{2-}, formed from SO_2 oxidation, and those surface SO_4^{2-} ions improved catalyst surface acidity, increased the adsorption of NH_3 and promoted NH_3 reaction with NO.

Once H_2O was inlet, the NO_x conversion over $VTiO_2$ declined sharply by more than 10%, as to VTNT-350, the conversion at 240 and 270 °C only fell by 5% and 2% or so, respectively. When H_2O was cut off, the catalytic activity in the above cases immediately recovered. With 4 vol% moisture content, water inhibition only had little impact on the catalytic activity over VTNT-350. Moreover, the inhibition was reversible and decreased with reaction temperature increasing. It didn't achieve an agreement on the inhibition mechanism of H_2O so far. Most researchers attributed water inhibition to the competitive adsorption with NO and/or NH_3 on active sites [40]. Others thought that H_2O inhibited the reaction of NO with adsorbed NH_3 [41]. According to our results, H_2O didn't involve in the SCR reaction, and we preferred to believe that it was the competitive physical adsorption of H_2O with reactants on catalyst surface that leaded to the reduction of NO_x conversion.

When the feed stream contained H_2O and SO_2 simultaneously, the catalytic activity in the above cases declined rapidly, and the NO_x conversion over VTNT-350 at 240 and 270 °C decreased to 62.70% and 82.02% from 73.36% and 94.41%, respectively. Subsequently, all the conversion increased slightly, followed by the slow reduction in the NO_x removal. After some time, the conversion over VTNT-350 at 240 and 270 °C stabilized around 57% and 78%, and for $VTiO_2$ the data floated around 28% and 49%, respectively. When the stream of H_2O and SO_2 ceased, the NO_x removal rebounded rapidly at first, and then declined swiftly. Finally, the NO_x conversion rose gradually. After lengthy recovery, the NO_x conversion still remained about 3% less than that before the aeration of H_2O and SO_2. The steep drop of the catalyst activity suggested a synergistic inhibitory effect of H_2O and SO_2, compared with the evolution when SO_2 or H_2O was added individually [37]. The sudden rebound before and after the aeration of H_2O and SO_2 demonstrated that the sulfate salts on catalyst surface were helpful to the NO_x reduction again. However, in the presence of H_2O, the deposition rate of sulfate species increased dramatically, and was far greater than the consumption rate. As a consequence, the sulfate salts not only deposited on the catalyst surface but also covered active center, and blocked catalyst pores and channels, causing decreasing in the NO_x conversion. Furthermore, H_2O competed with reactants by physical adsorption, further lowering the catalyst activity of VTNT-350.

When feeding SO_2 or H_2O to the reaction system individually, VTNT-350 exhibited higher tolerance to SO_2 and H_2O than $VTiO_2$. However, when SO_2 and H_2O was in the feeding stream simultaneously, the de-NO_x activity of VTNT-350 decreased continuously and took more time to recover. It could be attributed to the tubular structure of VTNT which was prone to blocking by deposited sulfate species.

CONCLUSION

The VTNT-350 exhibited significantly higher catalytic activity than the $VTiO_2$ in the broad temperature range of 120-300 °C. Characterization results indicated that the increase in catalytic activity was closely linked with the dispersion of V species on carriers. The good dispersion of V_2O_5 on TNT increased the surface acidity, which was beneficial to NH_3 adsorption, as well as to the increase of de-NO_x activity. Study on the resistance of VTNT-350 to SO_2 and H_2O showed that feeding SO_2 enhanced the NO_x removal efficiency, and H_2O inhibited the SCR reaction simply by competitive physical adsorption with NO. The synergistic effect of SO_2 and H_2O further decreased the denitration efficiency because of the competitive adsorption with reactive gas and the excessive deposition of ammonium sulfate into catalytic pores.

ACKNOWLEDGMENTS

This work was financially supported by the National Natural Science Foundation of China (51078185) and (U1162119), the research fund of Key Laboratory for Advanced Technology in Environmental Protection of Jiangsu Province (AE201001), Research Fund for the Doctoral Program of Higher Education of China (20113219110009), Industry-Academia Cooperation Innovation Fund Projects of Jiangsu Province (BY2012025) and Scientific Research Project of Environmental Protection Department of Jiangsu Province (201112).

REFERENCES

1. G. J. Lopez, G. Polupan, M. T. Velazquez and R. L. Leyte, *Appl. Therm. Eng.*, **29**, 1614 (2009).
2. X. L. Zhang, Z. G. Huang and Z. Y. Liu, *Catal. Commun.*, **9**, 842 (2008).
3. R. Q. Long and R. T. Yang, *Appl. Catal. B: Environ.*, **27**, 87 (2000).
4. H. Bosch and F. Janssen, *Catal. Today*, **2**, 369 (1988).

5. S. C. Wood, *Chem. Eng. Prog.*, **90**, 32 (1994).
6. M. F. H. V. Tol, M. A. Quinlan, F. Luck, G. A. Somorjai and B. E. Nieuwenhuys, *J. Catal.*, **129**, 186 (1991).
7. R. M. Heck, *Catal. Today*, **53**, 519 (1999).
8. R. Q. Long, R. T. Yang and R. Chang, *Chem. Commun.*, **57**, 452 (2002).
9. J. P. Chen, M. A. Buzanowski, R. T. Yang and J. E. Cichanowicz, *J. Air Waste Manage.*, **40**, 1403 (1990).
10. D. A. Pena, B. S. Uphade and P. G. Smirniotis, *J. Catal.*, **221**, 421 (2004).
11. Y. Huang, Z. Tong, B. Wu and J. F. Zhang, *J. Fuel. Chem. Technol.*, **36**, 616 (2008).
12. Q. Li, H. S. Yang, A. M. Nie, X. Y. Fan and X. B. Zhang, *Catal. Lett.*, **141**, 1237 (2011).
13. I. Giakoumelou, C. Fountzoula, C. Kordulis and S. Boghosian, *Catal. Today*, **73**, 255 (2002).
14. S. Higashimoto, W. Tanihata, Y. Nakagawa, M. Azuma, H. Ohue and Y. Sakata, *Appl. Catal. A: Gen.*, **98**, 104 (2008).
15. Y. T. Li and Q. Zhong, *J. Hazard. Mater.*, **172**, 635 (2009).
16. B. M. Reddy, B. Chowdhury and I. Ganesh, *J. Phys. Chem. B*, **102**, 10176 (1998).
17. B. M. Reddy, I. Ganesh and E. P. Reddy, *J. Phys. Chem. B*, **101**, 1769 (1997).
18. B. C. Huang, R. Huang, D. J. Jin and D. Q. Ye, *Catal. Today*, **126**, 279 (2007).
19. G. Marbán, R. Antuña and A. B. Fuertes, *Appl. Catal. B: Environ.*, **41**, 323 (2003).
20. R. Zanella, S. Giorgio, C. R. Henry and C. Louis, *J. Phys. Chem. B*, **106**, 7634 (2002).
21. S. A. Chen, J. N. Nian, C. C. Tsai and H. Teng, *J. Air Waste Manage. Assoc.*, **57**, 600 (2007).
22. A. Hinz, P. O. Larsson, B. Skaman and A. Andersson, *Appl. Catal. B: Environ.*, **34**,161 (2001).
23. L. Chmielarz, P. Kuœtrowski, R. Dziembaj, P. Cool and E. F. Vansant, *Appl. Catal. B: Environ.*, **62**, 369 (2006).
24. C. T. Hsieh, W. S. Fan, W. Y. Chen and J. Y. Lin, *Sep. Purif. Technol.*, **67**, 312 (2009).
25. T. Kasuga, M. Hiramatsu, A. Hoson, T. Sekino and K. Niihara, *Langmuir.*, **14**, 3160 (1998).
26. G. H. Du, Q. Chen, R. C. Che, Z. Y. Yuan and L. M. Peng, *Appl. Phys. Lett.*, **79**, 3702 (2001).
27. Q. Chen, W. Zhou, G. H. Du and L. M. Peng, *Adv. Mater.*, **14**, 1208 (2002).
28. X. Y. Kong, Y. Ding, R. Yang and Z. L. Wang, *Science*, **303**, 1348 (2004).
29. D. A. Wang, F. Zhou, Y. Liu and W. M. Liu, *Mater. Lett.*, **62**, 1819 (2008).
30. Z. H. Zhao, J. M. Fan, J. Y. Wang and R. F. Li, *Catal. Commun.*, **21**, 32 (2012).
31. B. X. Shen, Y. Yao, H. Q. Ma and T. Liu, *Chin. J. Catal.*, **32**, 1803 (2011).
32. X. L. Yin, H. M. Han, I. Gunji, A. Endou, S. S. C. Ammal, M. Kubo and A. Miyamoto, *J. Phys. Chem. B*, **103**, 4701 (1999).
33. G. Ramis, Y. Li, G. Busca, M. Turco, E. Kotur and R. J. Willey, *J. Catal.*, **157**, 523 (1995).
34. Q. Y. Liu, Z. Y. Liu and C. Y. Li, *Chin. J. Catal.*, **27**, 636 (2006).
35. H. T. Xu, Y. S. Shen, C. H. Shao, F. W. Lin, S. M. Zhu and T. Xiu, *J. Rare Earth.*, **28**, 721 (2010).
36. L. H. Dong, C. Z. Sun, C. J. Tang, B. Zhang, J. Zhu, B. Liu, F. Gao, Y. H. Hu, L. Dong and Y. Chen, *Appl. Catal. A: Gen.*, **431**, 126 (2012).
37. S. L. Zhang, H. Y. Li and Q. Zhong, *Appl. Catal. A: Gen.*, **435**, 156 (2012).
38. R. Q. Long and R. T. Yang, *J. Catal.*, **207**, 158 (2002).
39. Z. P. Zhu, Z. Y. Liu, S. J. Liu and H. X. Niu, *Appl. Catal. B: Environ.*, **23**, 229 (1999).
40. J. Muòiz, G. Marbán and A. B. Fuertes, *Appl. Catal. B: Environ.*, **27**, 27 (2000).
41. I. Nova, L. Lietti, E. Tronconi and P. Forzatti, *Catal. Today*, **60**, 73 (2000).